

Scientific paper

### Eco-friendly Synthesis, Characterization, and Biological Evaluation of Silver Nanoparticles from Verbascum uschakense Aqueous Extract

Mürüvvet Kurt<sup>1,\*</sup> o and Funda Çet<sup>1</sup> o

<sup>1</sup> Department of Chemistry, Afyon Kocatepe University, Afyonkarahisar, Turkey

\* Corresponding author: E-mail: muruvvetkurt@aku.edu.tr and duzmuruvvet@gmail.com

Received: 11-11-2024

#### **Abstract**

Silver nanoparticles synthesized using *Verbascum uschakense* extract at a reaction temperature of 60 °C were characterized through multiple analytical techniques. These included ultraviolet-visible absorption spectroscopy, X-ray diffraction analysis, high-resolution transmission electron microscopy, and scanning electron microscopy coupled with energy dispersive X-ray spectroscopy. Ultraviolet-visible spectral analysis revealed a surface plasmon resonance peak at 432 nanometers, indicating the successful formation of silver nanoparticles. Microscopic analyses demonstrated that the nanoparticles were predominantly spherical in shape, with particle sizes ranging between 4 and 14 nanometers. X-ray diffraction analysis confirmed that the silver nanoparticles possessed a face-centered cubic crystal structure, as evidenced by characteristic diffraction peaks at  $2\theta$  values of  $38.21^\circ$ ,  $44.46^\circ$ ,  $64.59^\circ$ , and  $77.48^\circ$ , corresponding to the (111), (200), (220), and (311) planes, respectively.

Regarding the biological activities, the antioxidant capacity of the aqueous extract of *V. uschakense* was evaluated by its ability to scavenge free radicals. At a concentration of 1 milligram per milliliter, the extract demonstrated a 86.93 percent scavenging effect against the stable radical 2,2-diphenyl-1-picrylhydrazyl. In comparison, the silver nanoparticles synthesized from the plant extract exhibited a 60.04 percent scavenging effect at the same concentration. Additionally, the silver nanoparticles showed strong inhibition in the 2,2'-azino-bis(3-ethylbenzothiazoline-6-sulfonic acid) radical scavenging assay, with values comparable to those obtained using the standard antioxidant TroloxThe antimicrobial properties of the biosynthesized silver nanoparticles were examined using the disc diffusion method. The nanoparticles exhibited inhibitory activity against several pathogenic microorganisms, including *Staphylococcus aureus*, *Streptococcus mutans*, *Escherichia coli*, *Pseudomonas aeruginosa*, *Listeria monocytogenes*, and fungal species belonging to the *Candida* genus.

These results highlight the potential of *V. uschakense*-mediated silver nanoparticles as multifunctional bioactive agents with both antioxidant and antimicrobial properties. The study demonstrates that green synthesis offers a sustainable and effective approach to producing nanomaterials with potential applications in biomedical and pharmaceutical fields.

Keywords: Green synthesis, Silver nanoparticle characterization, Antioxidant activity,

#### 1. Introduction

Nanotechnology has made revolutionary advancements in various industrial and scientific fields in recent years. Nanoparticles (NPs) possess unique physicochemical properties due to their specific sizes, shapes, compositions, and high surface area-to-volume ratios.<sup>1,2</sup> These properties enable NPs to be used in a wide range of applications, including antimicrobial, anticancer, anti-inflammatory, surfactant, and drug delivery systems. However, traditional physical and chemical synthesis methods often

result in high costs and the production of toxic by-products.<sup>3</sup>

Green synthesis methods are emerging as an eco-friendly alternative to overcome these issues.<sup>4</sup> NPs produced from biological materials are known as biogenic NPs, and the related synthesis process is referred to as green synthesis. The green synthesis of NPs involves the use of prokaryotic/eukaryotic cells or extracted biomolecules that act as reducing agents.<sup>4</sup> Plant biomass/extract offers several advantages over other microscopic organisms for NP synthesis due to its diverse biological mate-

rials. The biosynthesis of metallic NPs using plants occurs through biomolecules present in plant biomass, which contain organic functional groups.<sup>5</sup>

Moreover, recent reviews have underscored the biomedical promise of silver and gold nanoparticles synthesized via green routes, particularly due to their high biocompatibility and antimicrobial efficacy.<sup>6</sup>

Similarly, microbial-mediated synthesis approaches have also shown significant antibacterial potential, as evidenced by the biosynthesis of AgNPs using *Lactobacillus* and *Bacillus* species, supporting the diversity of biological agents usable in eco-friendly nanomaterial production.

Verbascum species are plants with many therapeutic uses in traditional medicine. They are particularly known for their expectorant, diuretic, soothing, demulcent, and sedative effects, as well as their antiviral, antibacterial, antifungal, cytotoxic, and antitumor activities. These properties necessitate detailed bioactivity and chemical composition studies of Verbascum species. Research has shown that the Verbascum genus contains various secondary metabolites, such as iridoid glycosides, triterpenic saponins, and flavonoids. These active compounds provide strong biological activities that support the potential medicinal applications of these plants.

In recent years, there has been a notable rise in research exploring plant-derived gold nanoparticles as carriers for therapeutic agents, which further emphasizes the significance of exploring medicinal plants such as *Verbascum* spp. for similar nanomedical applications.<sup>11</sup>

While several Verbascum species have been studied for their phytochemical composition and biological activities, there is currently a significant lack of research regarding V. uschakense, an endemic species of Turkey. The novelty of this study lies in its focus on this underexplored species, thereby addressing a notable gap in the existing literature. Recent studies have emphasized the increasing interest in exploring lesser-known Verbascum taxa for nanoparticle-based biomedical applications. 12-14 However, to our knowledge, this is the first report on the use of V. uschakense in the green synthesis of silver nanoparticles. This study not only contributes to the growing field of green nanotechnology but also adds new insights into the potential applications of endemic flora in nanomedicine. Such studies are essential for broadening the chemotaxonomic understanding of the genus and for identifying novel bioresources for eco-friendly nanomaterial production. This study involves the green synthesis of silver nanoparticles (AgNPs) using the aqueous extract of the aerial parts of V. uschakense, an endemic species growing in Turkey, which has not yet been studied in terms of its chemical composition and bioactivity in the literature. The antibacterial and antioxidant activities of these nanoparticles were also evaluated. This research aims to provide valuable insights into the potential medicinal applications of V. uschakense and the biological activities of silver nanoparticles produced through green synthesis methods.

#### 2.Experimental

### 2. 1. Collection and Identification of Plant Materials

*V. uschakense* (Murb) Hub.-Mor. was collected from B3 Afyon – Central Northeast, steppe, at an altitude of 1020 meters by Prof. Dr. Mustafa Kargıoğlu and identified. The plants were cut into small pieces and dried in the shade at room temperature.

### 2. 2. Preparation of Plant Extracts in the Laboratory

Fresh leaves of *V. uschakense* were first cleaned with tap water and then rinsed with deionized water. After air-drying in the shade for 2–3 days, the leaves were pulverized into a fine powder using an electric blender. A total of 10 g of the powdered leaves was mixed with 200 mL of distilled water and heated to 70–80 °C while stirring for 30 minutes using a magnetic stirrer. The resulting extract was filtered through Whatman Grade 1 filter paper, allowed to cool, and stored at 4 °C in a refrigerator. <sup>15–16</sup> Additionally, Soxhlet extraction was employed to obtain further plant extracts, which were then used for antioxidant activity analysis.

#### 2. 3. Green Synthesis of Silver Nanoparticles

Silver nitrate (AgNO<sub>3</sub>) solutions with concentrations of 0.1 mM, 1 mM, and 5 mM were prepared by dissolving AgNO<sub>3</sub> crystals in deionized water. These solutions were mixed with the V. uschakense extract in a 1:10 (v/v) ratio (e.g., 5 mL AgNO<sub>3</sub> solution to 45 mL plant extract), making a total reaction volume of 50 mL. 17 The mixture was transferred into a glass reaction container wrapped in aluminum foil to protect it from light and was left undisturbed at room temperature (25  $\pm$  2 °C) until a visible color change from yellow to dark brown was observed, which typically occurred within 24 hours, indicating the formation of silver nanoparticles. After the reaction, the solution was centrifuged at 5000 rpm for 20 minutes. The supernatant was discarded, and the precipitate was washed with 5 mL of deionized water twice, followed by a final wash with ethanol. The resulting pellet was dried in an oven at 60 °C for 30 minutes. The synthesized nanoparticles were referred to as VUAgNPs.

## 2. 4. Characterization of Synthesized Nanoparticles

The silver nanoparticles synthesized via green synthesis were examined using both macroscopic and microscopic analysis techniques. During the reaction process, the color change from yellow to brown in the plant extract was observed. The surface plasmon resonance peak indicating the formation of AgNPs was monitored using a

UV-1700 PHARMA SPEC brand UV-vis spectrophotometer. The size and structural properties of the nanoparticles were analyzed using a JEOL JEM-1400 PLUS model transmission electron microscope (TEM). XRD analyses were conducted on a PANalytical Empyrean device using at least 0.1 g of sample. Additionally, imaging was performed using a LEO 1430 VP model scanning electron microscope (SEM) and an energy-dispersive X-ray spectroscopy (EDX) detector, specifically the RÖNTEC QX2 model XFlash type X-ray detector.

### 2. 5. Antioxidant Activity Tests of Silver Nanoparticles

### 2. 5. 1. DPPH Free Radical Scavenging Activity Method

The free radical scavenging activities of silver nanoparticles obtained using plant extract and aqueous fraction were analyzed using the DPPH free radical method. Samples prepared at concentrations of 0.0625, 0.125, 0.25, 0.5, and 1 mg/mL were added to microplates in a volume of 40  $\mu L$ , followed by the addition of 160  $\mu L$  of DPPH solution. For the control group, 40  $\mu L$  of ultra-pure water was used instead of the sample. After incubating the mixtures at room temperature for 30 minutes, the absorbance values were measured at 517 nm. These values were evaluated by comparing them with the control. BHA and GA were used as standards. The free radical scavenging activity was determined using the following formula:

% DPPH Inhibition = 
$$[(A_0-A_1)\,/\,A_0]\times 100$$

where  $A_0$  is the absorbance of the control group, and  $A_1$  is the absorbance of the samples.<sup>19</sup> The % inhibition rates were calculated using the data obtained from these absorbance values.<sup>20</sup> All experiments were performed in triplicate and the results were expressed as mean  $\pm$  standard deviation.

### 2. 5. 2. Evaluation of Antioxidant Activity Using the ABTS<sup>+</sup> Radical Cation Method

The antioxidant activity of both the plant extract and VUAgNPs was evaluated using the ABTS<sup>+</sup> radical cation decolorization method, as outlined by Thaipong et al. This technique involves the inhibition of the ABTS<sup>+</sup> radical cation, which is produced through an oxidation reaction involving 2,2'-azino-bis (3-ethylbenzothiazoline-6-sulfonic acid) and potassium persulfate ( $K_2S_2O_8$ ). A 2.6 mM potassium persulfate solution and a 7.4 mM ABTS<sup>+</sup> solution were prepared as stock solutions. The working solution was created by combining equal volumes (1:1) of both stock solutions, followed by incubation in the dark at room temperature for 16

hours. Afterward, the ABTS<sup>+</sup> solution was diluted with methanol to achieve an absorbance of 1.1  $\pm$  0.02 units at 734 nm (1:80). Then, 150  $\mu L$  of the sample was mixed with 2850  $\mu L$  of the freshly prepared ABTS<sup>+</sup> solution and incubated in the dark for 6 minutes. The absorbance was then measured at 734 nm. Trolox was used as the standard solution in this assay. The ABTS<sup>+</sup> radical inhibition percentage was determined using the equation below:

Inhibition (%) = 
$$[(A_{control} - A_{sample}) / A_{control}] \times 100$$

 $A_{
m control}$ : Absorption obtained by adding solvent instead of sample  $A_{
m sample}$ : Absorbance of sample All experiments were performed in triplicate and the results were expressed as mean  $\pm$  standard deviation.

## 2. 6. Antibacterial Activity of Silver Nanoparticles

The microorganisms used for the antimicrobial activity study (*P. aeruginosa* ATCC 27853, *E. coli* ATCC 25922, *S. aureus* ATCC 25923, *Staphylococcus mutans*, *Listeria monocytogenes*, *Candida* sp) were obtained from the culture collection of Uşak University Vocational School of Health Services.

The antimicrobial activity of VUAgNPs was evaluated against fungi and bacteria using the agar well diffusion method. Under sterile conditions, wells were created on Müller Hinton Agar (Merck, 105437) (MHA), and 50  $\mu L$  of the extract was added to each well. Bacterial cultures, which were incubated overnight, were diluted with sterile water to a turbidity standard of 0.5 McFarland at 600 nm, and streak inoculations were performed at a right angle to the wells. After incubation at 37  $\pm$  2 °C for 24 hours, the zone of inhibition, where bacterial growth had begun, was measured in millimeters.

#### 2. 7. Antifungal Activity

The fungi used for the antifungal activity study (*Penicillium citrinum* NRRL174127, *Aspergillus flavus* NRRL980, *Fusarium solani* NRRL13414, *Aspergillus niger* 1094) were obtained from the culture collection of Uşak University Vocational School of Health Services.

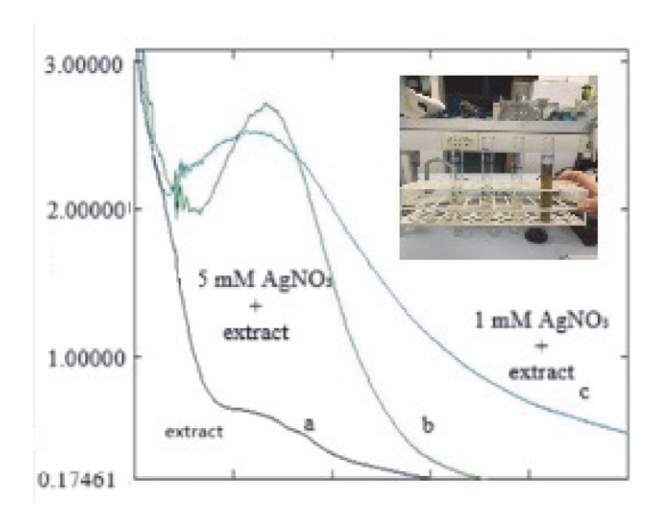
A 1 cm agar disk was removed from the center of Petri dishes containing PDA. 50 mL of solvent and test material samples were separately added to these wells. The samples were taken from the outer edges of the fungal colony types. After this step, they were inoculated onto PDA plates at equal distances from the center wells. The plates were incubated in the dark at 27 °C for 7 days. The distance of the fungal hyphae from the center well was measured in millimeters. The percentage inhibition of mycelial growth was calculated by comparing it with the control.

#### 3. Results And Discussion

## 3. 1. Characterization of Synthesized Nanoparticles

#### 3. 1. 1. UV-Visible Spectroscopy Analysis

Due to the interaction of VUAgNPs with mobile surface electrons, a significant reaction known as surface plasmon resonance (SPR) occurs in the range of 400–500 nm, resulting in a transformation from a pale yellow to a brown colloidal solution. This color change allows for the qualitative detection of AgNPs, and it has been reported that the increase in concentration of AgNPs over time is due to the SPR on their surfaces.<sup>22</sup>



colloidal formation also support this result; silver nanoparticles typically exhibit a yellowish-brown color, which correlates with the SPR peak.<sup>26</sup>

The morphology of silver nanoparticles can vary depending on the synthesis conditions, which also affects the SPR values determined by UV-Vis spectroscopy. Sun et al. demonstrated that the UV-Vis absorbance of silver nanoparticles is generally in the 400–450 nm range and that there is a strong relationship between nanoparticle size and spectral position. Jain et al. emphasized that the SPR peaks vary depending on the shapes and sizes of silver nanoparticles and that optical properties can be controlled. Additionally,

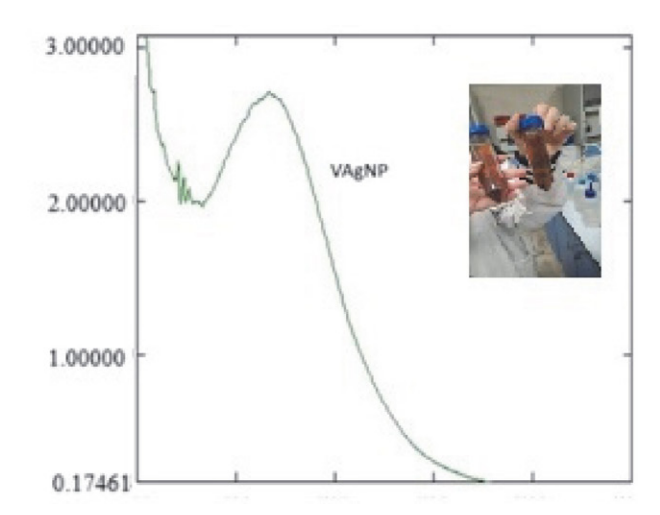


Figure 1. UV–Vis absorption spectra of silver nanoparticles synthesized using *V. uschakense* aqueous extract. The spectra correspond to: (a) plant extract, (b) 5 mM AgNO<sub>3</sub>, and (c) 1 mM AgNO<sub>3</sub>. The 0.1 mM AgNO<sub>3</sub> sample was excluded due to the absence of a SPR peak. A more intense and sharper SPR band was observed at 5 mM, indicating enhanced nanoparticle formation at higher precursor concentration.

The color change observed in our study and the data showing a maximum absorbance of 432 nm for VUAgNPs in UV-Vis measurements support this formation (Figure 1). In UV-Vis analysis, a distinct SPR peak in the range of 400-500 nm is expected during the characterization of silver nanoparticles. In this study, the maximum absorbance peak at 432 nm is consistent with values reported in the literature. It is particularly thought that the peak obtained in the range of 400-450 nm indicates that the nanoparticles were synthesized in a small size and uniformly.<sup>23</sup> The SPR property of AgNPs arises from the interaction of mobile electrons on the surface of metal nanoparticles with light, and this interaction is used as a fundamental indicator in the study of the optical properties of nanoparticles.<sup>24</sup>

The emergence of a surface plasmon resonance (SPR) peak around 432 nm suggests that the silver nanoparticles are likely spherical or near-spherical in shape and range in size from approximately 10 to 50 nm, which is consistent with previously reported size distributions and characteristic SPR features for VUAgNPs.<sup>20–25</sup> Additionally, macroscopic observations such as color change and

Sharma et al.<sup>29</sup> pointed out the effects of environmental conditions and synthesis methods on SPR, noting that silver nanoparticles have a broad-spectrum antimicrobial effect.

### 3. 1. 2. Scanning Electron Microscopy and Energy Dispersive X-ray Spectroscopy (SEM-EDX)

Elemental analyses of silver nanoparticles were conducted using an Energy Dispersive X-ray device integrated with an electron microscope. Figure 2 presents the SEM images of VUAgNPs samples and the results of the EDX analysis. SEM-EDX spectroscopy was utilized to confirm the formation of pure silver or silver oxide particles in the elemental composition. In various studies, the observation of an ~3 keV optical absorption peak in the formation of AgNPs has been indicated to be due to the surface plasmon resonance of silver nanoparticle extracts. <sup>30</sup>

SEM images provide important insights into the morphology and distribution of nanoparticles. The SEM images presented in this study indicate that the AgNPs

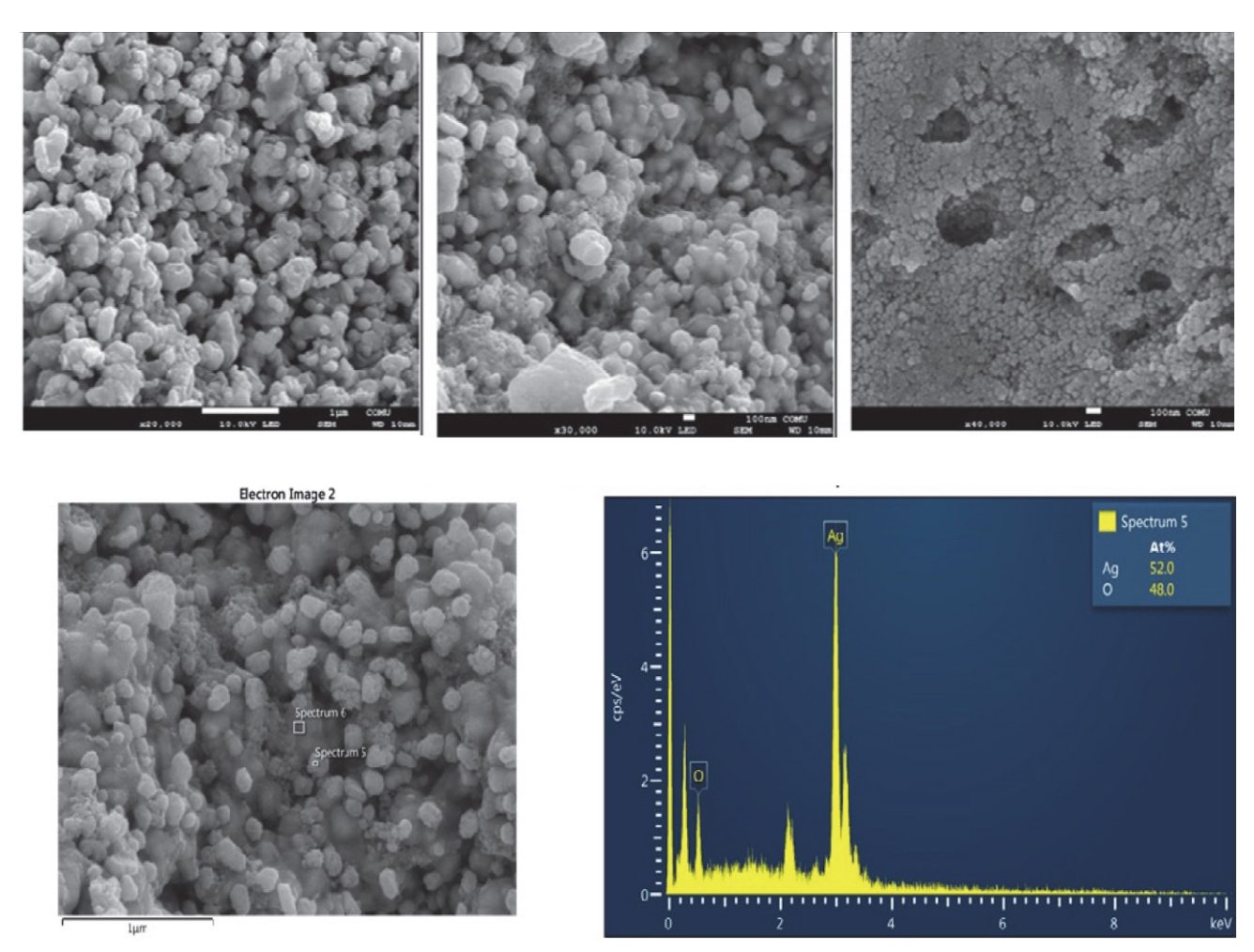


Figure 2. SEM image and EDX analysis result of the VUAgNPs sample.

generally possess a spherical or near-spherical structure. This is consistent with the morphology of AgNPs commonly observed in the literature.<sup>23</sup> Silver nanoparticles typically exhibit a homogeneous structure, with sizes generally ranging from 10 to 100 nm. This size range is also compatible with the SPR peak observed at 432 nm obtained from UV-Vis spectroscopy.

EDX analysis confirms the elemental composition of the nanoparticles in addition to the visual information obtained from the SEM images. The Ag (silver) peak observed in the EDX analysis of this study proves that the nanoparticles are composed of pure silver. This finding indicates that pure silver nanoparticles were obtained during the synthesis process and that no contamination occurred. These results are in parallel with the studies conducted by Alanazi et al.<sup>30</sup>

The other elements observed in the EDX analysis (such as oxygen) may indicate oxidation occurring on the surface of the nanoparticles or the presence of stabilizing agents. The presence of such elements can enhance the long-term stability of the nanoparticles and their potential in biomedical applications.<sup>28</sup>

#### 3. 1. 3. Transmission Electron Microscopy (TEM)

The structural characterization of the synthesized silver nanoparticles and their size analysis, as shown in Figure 4, indicates that spherical nanoparticles (4–14 nm) were obtained for VUAgNPs.

According to the results of TEM, the synthesized silver nanoparticles are observed to be in the size range of 4-14 nm and exhibit a spherical morphology. (Figure 3). In addition to the prominent peaks corresponding to silver (Ag) and oxygen (O), minor peaks were observed at approximately 0.25 keV (C), 1.5 keV (Al), 1.74 keV (Si), and 2.3 keV (S), which may originate from the sample holder materials (e.g., carbon tape or copper grid), residual compounds from the synthesis process, or environmental contamination. The characteristic Ag peaks, including both low-energy (Lα/Lβ) and high-energy (Kα at ~8.04 keV) signals, confirm the presence of silver nanoparticles. The peak observed near 8.9 keV may be attributed to the Ag Kβ line or could overlap with the Cu Ka peak from the copper grid used during analysis. These findings indicate that the methods used during nanoparticle synthesis are effective in achieving size

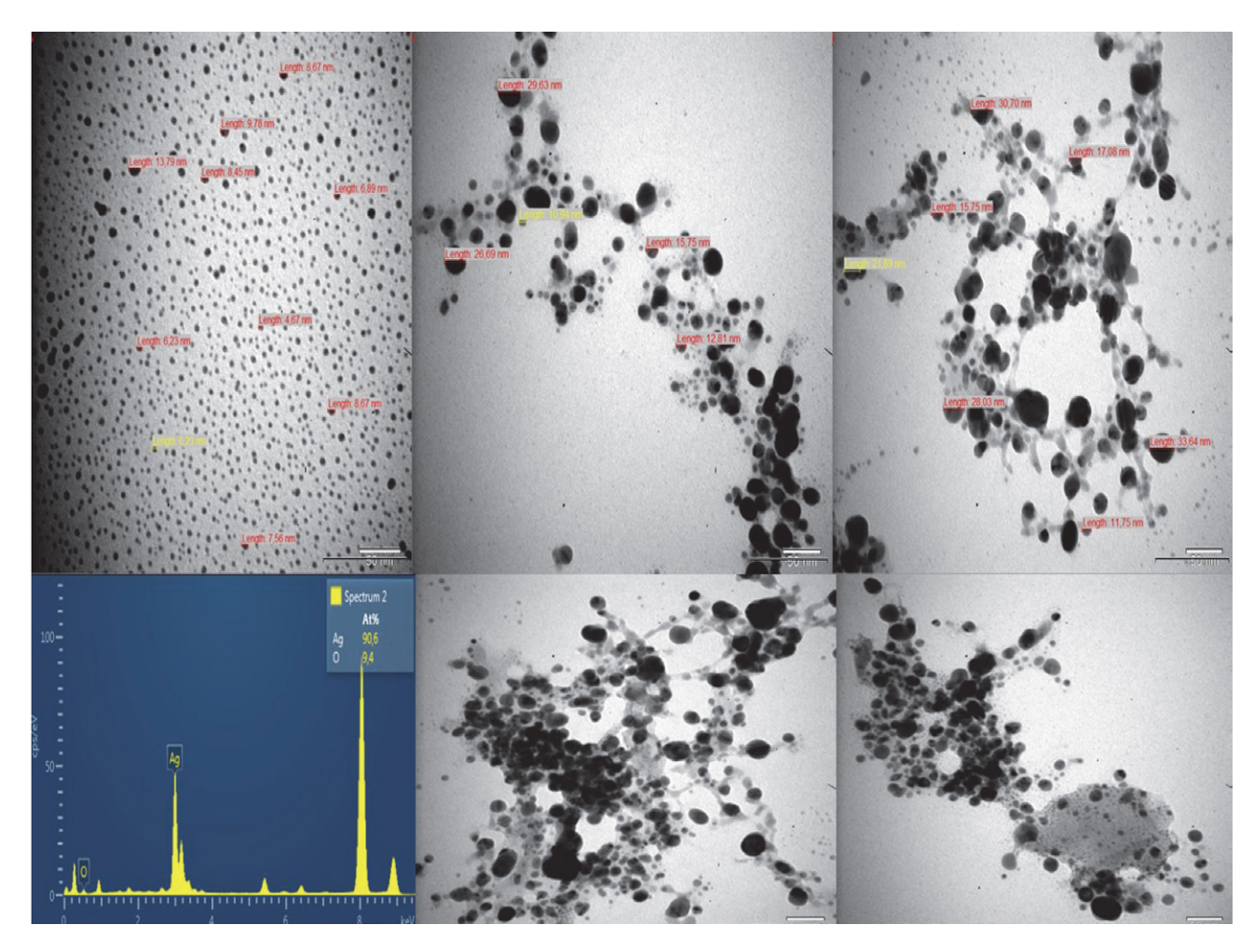


Figure 3. TEM-EDX spectrum of the synthesized silver nanoparticles.

control and homogeneous particle shape. The small size of the nanoparticles generally indicates a larger surface area and consequently a more active surface chemistry, which provides significant advantages in biological and catalytic applications. The attainment of a spherical structure can enhance the stability and dispersibility of the particles, which is a critical factor, especially in biomedical applications (for example, in drug delivery systems or as antimicrobial agents). These results are consistent with other studies in the literature; for instance, it has been reported that silver nanoparticles synthesized in similar size ranges optimize antimicrobial activity and significantly improve optical properties such as surface plasmon resonance. In this context, the findings obtained from the TEM analysis provide strong insights into the potential applications of these particles. Various studies have reported that silver nanoparticles are typically in spherical form and in the size range of 5-50 nm. For example, Sotiriou and Pratsinis<sup>31</sup> obtained spherical silver nanoparticles with diameters of 20-40 nm and noted that the surface plasmon resonance properties of these particles are directly related to their size. Similarly, Ahamed et al.<sup>32</sup> detected the sizes of synthesized silver nanoparticles in

the range of 10–25 nm through TEM images and stated that the particles are highly monodispersed.

#### 3. 1. 4. X-ray Diffraction Analysis (XRD)

XRD is employed to investigate the particle size, phase composition, and crystal structure of VUAgNPs synthesized through the green synthesis approach, with particle sizes ranging between 5 and 40 nm.<sup>33</sup> (Figure 4). In the research by Bagherzade et al.<sup>34</sup> the XRD pattern of synthesized AgNPs showed four distinct diffraction peaks at  $2\theta$  values of  $38.35^{\circ}$ ,  $46.46^{\circ}$ ,  $64.75^{\circ}$ , and  $77.62^{\circ}$ , corresponding to the characteristic Bragg planes (111), (200), (220), and (311) of the face-centered cubic (FCC) structure.

In this study, the XRD data of the synthesized VUAg-NPs reveal peaks at  $2\theta = 38.21^{\circ}$ ,  $44.46^{\circ}$ ,  $64.59^{\circ}$ , and  $77.48^{\circ}$ , which correspond to the Bragg reflections of the (111), (200), (220), and (311) planes, respectively. These peaks match well with the standard data for crystalline silver (JCPDS Card No. 04–0783), confirming the formation of a face-centered cubic structure. The absence of additional impurity peaks indicates high purity of the synthesized

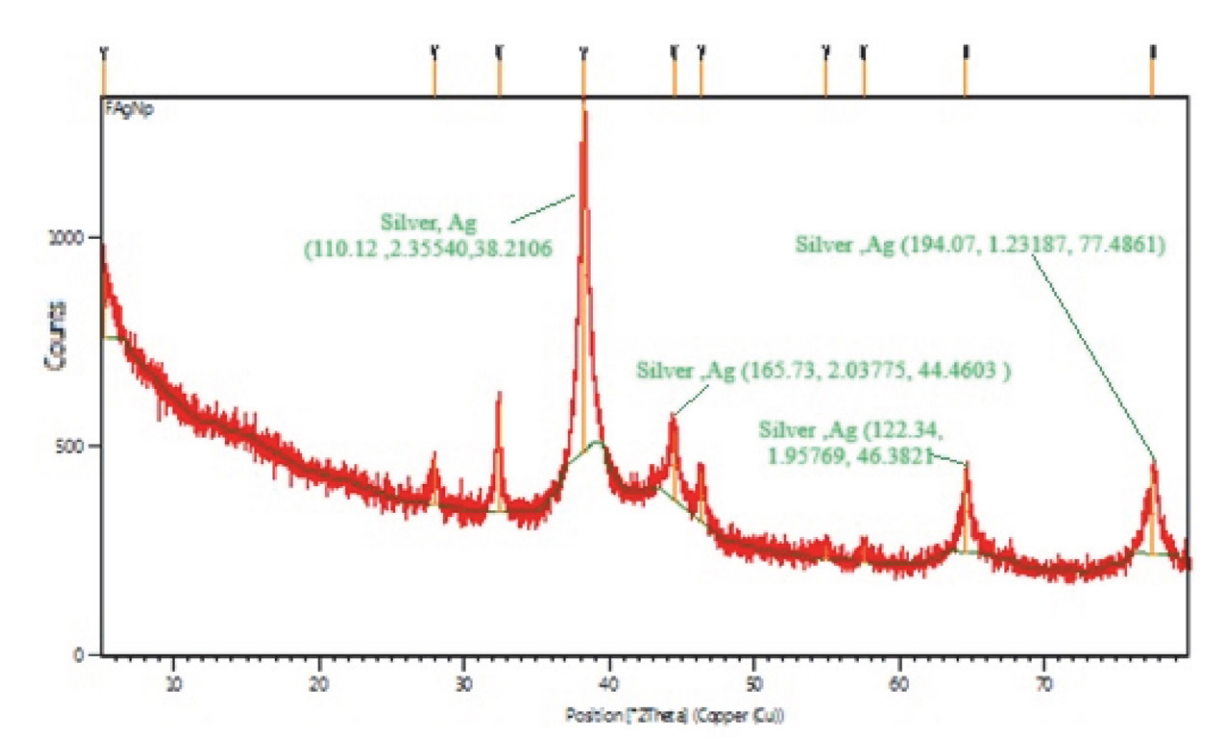


Figure 4. XRD results of the VUAgNPs sample.

nanoparticles. The data suggest that the AgNPs possess an elemental silver (Ag<sup>0</sup>) composition and exhibit a predominantly spherical crystalline morphology.

## 3. 2. Antioxidant Activity Tests of Silver Nanoparticles

#### 3. 2. 1. DPPH Free Radical Scavenging Capacity

The DPPH free radical scavenging capacity of *V. us-chakense* extract and nanoparticles is shown in Figure 5.

The measurements, conducted at concentrations of 0.0625, 0.125, 0.25, 0.5, and 1 mg/mL, showed a dose-dependent increase in absorbance.

In a study by Imtiaz et al.<sup>35</sup> AgNPs synthesized from *Piper longum* fruit extract exhibited an average inhibition of approximately 67%, which was lower than both the standard and fruit extract (~80%). In the present study, the DPPH scavenging activity of VUAgNPs was observed to be lower than the standard antioxidant BHA. Additionally, another investigation noted that the inhibition capacity of AgNPs increased with concentration, with the

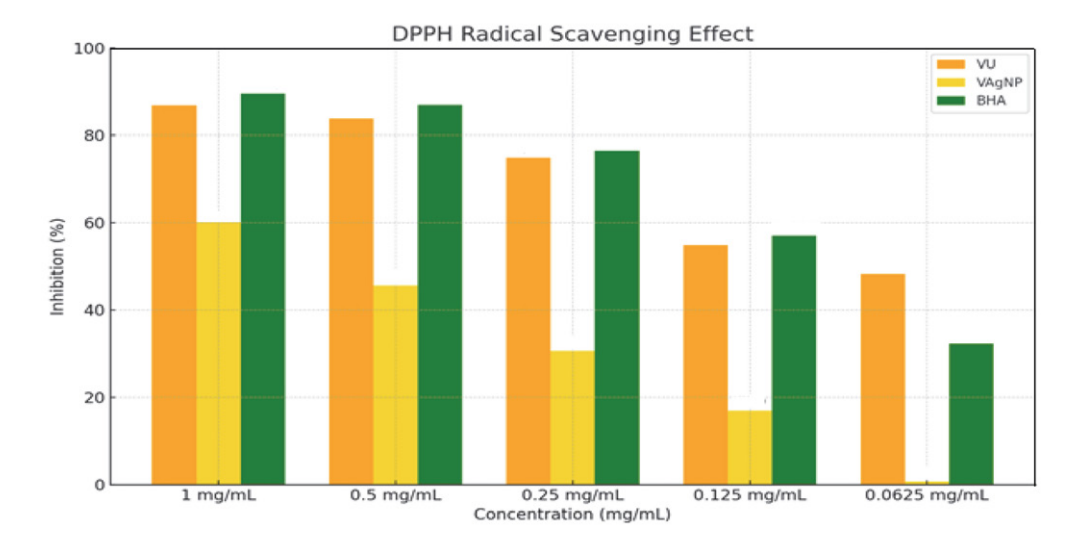


**Figure 5.** Radical Scavenging Effect of VU and VUAgNPs on DPPH.

VU: (*V. uschakense* plant extract); VUAgNPs: Silver nanoparticles obtained through green synthesis from the extract.

highest DPPH activity recorded at 100 mg/mL reaching  $55.84 \pm 1.31\%$ . In our experiment, the *V. uschakense* extract showed a DPPH free radical scavenging capacity of 86.93% at 1 mg/mL, whereas VAgNP exhibited 60.04%. Notably, the plant extract demonstrated a stronger DPPH radical scavenging effect compared to the silver nanoparticles.

Silver nanoparticles interact with free radicals and release hydrogen, converting them into more stable products.<sup>37</sup> This mechanism explains the lower antioxidant activity of silver nanoparticles in comparison to the plant extract. Similar findings were reported by Balkan et al.<sup>38</sup> and Küp et al.<sup>39</sup> in their respective studies.

# 3. 2. 2. Radical Cation Test with 2,2'-azino-bis (3-ethylbenzothiazoline-6-sulfonic acid) (ABTS)

The ABTS cation radical scavenging capacities of *V. uschakense* plant extract (VU) and the silver nanoparticles (VUAgNPs) synthesized from this extract using a green synthesis method were investigated at five different concentrations (1 mg/ml, 0.5 mg/ml, 0.25 mg/ml, 0.125 mg/ml, 0.0625 mg/ml). Trolox was used as a standard. At a concentration of 1 mg/ml, VAgNP and Trolox exhibited nearly the same level of radical scavenging capacity, with inhibition values of 83.48% and 83.23%, respectively. However, the inhibition of VU was significantly lower at 43.30% (Figure 6)

The ABTS cation radical scavenging activity of VUAgNPS is quite close to that of Trolox at higher concentrations (1 mg/ml and 0.5 mg/ml). Specifically, at a concentration of 1 mg/ml, VUAgNPs exhibited an inhibition value nearly equivalent to that of Trolox (83.48% and 83.23%). This indicates, as previously mentioned in the

literature.<sup>40</sup> That silver nanoparticles possess very strong antioxidant properties. Although these nanoparticles show a decrease in inhibition capacity as the concentration decreases, they still demonstrated similar performance to Trolox even at a concentration of 0.0625 mg/ml.

The plant extract has a lower radical scavenging capacity and exhibits significantly lower inhibition values compared to the nanoparticles, especially at concentrations of 1 mg/ml and 0.5 mg/ml. The lower inhibition of the plant extract compared to the nanoparticles supports the finding that silver nanoparticles, which have a high surface area and nanoparticle sizes, enhance antioxidant capacity.<sup>41</sup>

The discrepancy observed between the results of the DPPH and ABTS assays can be attributed to the differences in radical species, solvent solubility, and underlying reaction mechanisms of the two methods. The DPPH radical is lipophilic and primarily soluble in organic solvents, whereas the ABTS radical is soluble in both aqueous and organic media, making it more reactive toward both hydrophilic and lipophilic antioxidants. In our study, the enhanced ABTS radical scavenging activity of the hydrophilic silver nanoparticles (VUAgNPs) may be due to this compatibility in the aqueous medium.

Moreover, the DPPH assay predominantly involves a hydrogen atom transfer (HAT) mechanism, while the ABTS assay operates through both hydrogen atom transfer and electron transfer (ET) mechanisms.<sup>13</sup> This dual mechanism in ABTS could explain the higher reactivity of silver nanoparticles in this assay, as also supported by previous studies reporting that the high surface area and energy of nanoparticles enhance their antioxidant interactions. <sup>38–39</sup> Consistently, in our results, while VUAgNPs exhibited lower inhibition values in the DPPH assay compared to the plant extract, they showed comparable activ-

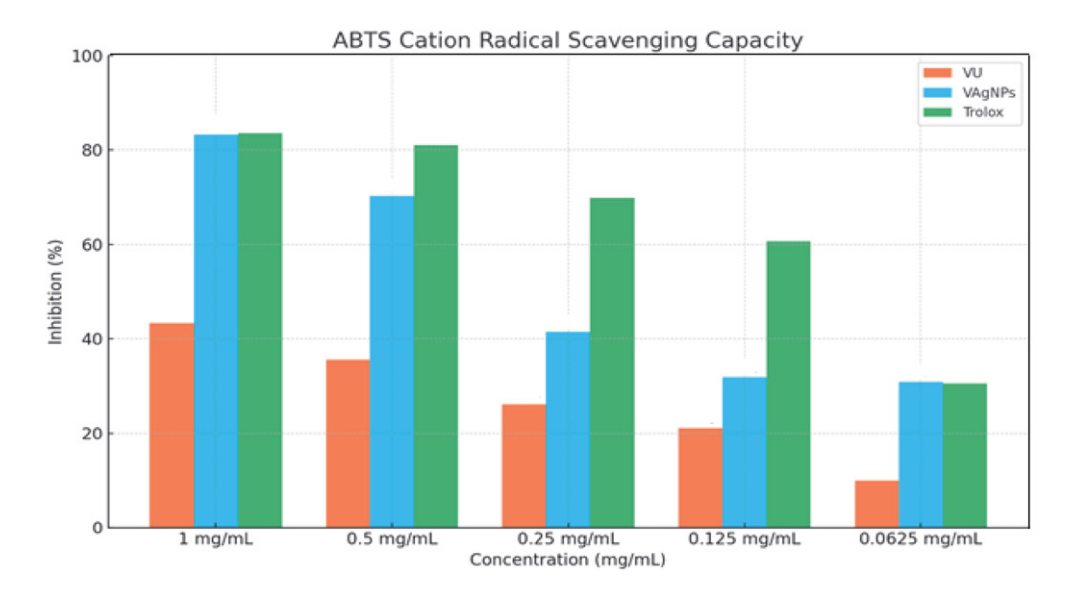


**Figure 6.** The ABTS cation radical scavenging capacities of VU and VUAgNPs. VU: (*V. uschakense* plant extract); VAgNP: Silver nanoparticles obtained from the extract using the green synthesis method.

ity to Trolox in the ABTS assay. These findings underline the complementary nature of both methods and highlight the importance of employing multiple assays to obtain a comprehensive assessment of antioxidant capacity.

## 3. 3. Determination of the Antibacterial Activity of Silver Nanoparticles

In our study, VUAgNPs completely inhibited the growth of *Listeria monocytogenes*. It exhibited the highest antimicrobial activity against *Staphylococcus aureus* (10 mm), followed by *Pseudomonas aeruginosa* (5 mm) and *Staphylococcus mutans* (5 mm). VUAgNPs inhibited the mycelial growth of *Aspergillus niger* by 6.66%. Additionally, it inhibited the mycelial growth of *Fusarium solani* NRRL13414 by 68.75%, while inhibiting *Aspergillus flavus* NRRL980 mycelial growth by 44.44%.

The antimicrobial effects of AgNPs are generally based on various mechanisms, such as the production of reactive oxygen species (ROS), damage to the cell membrane, and inhibition of DNA and protein synthesis. <sup>42</sup> The bacterial inhibition zones observed in this study indicate that AgNPs weaken the survival abilities of these pathogens by disrupting the cell membrane and releasing silver ions. These mechanisms have been widely discussed in the literature and are supported by findings that emphasize the difficulty of developing resistance due to the multiple modes of action of AgNPs. <sup>43</sup>

AgNPs are known for their potent antimicrobial properties, attributed to their small size and large surface area. This study observed complete inhibition of *Listeria monocytogenes* growth, aligning with previous research that high-

lights AgNPs strong activity against Gram-positive bacteria. Despite their thick peptidoglycan layers, these bacteria can be penetrated by silver nanoparticles, which bind to the cell membrane and disrupt internal cellular structures. 42-44 A 10 mm inhibition zone observed against *Staphylococcus aureus* further emphasizes the effectiveness of AgNPs against Gram-positive strains, which is well-documented in the literature In addition, inhibition zones of 5 mm against *Staphylococcus mutans* and *Pseudomonas aeruginosa* suggest that AgNPs could also inhibit Gram-negative bacteria. Notably, *Pseudomonas aeruginosa*, which is resistant to multiple drugs, was also inhibited by AgNPs, pointing to a potential alternative mechanism of action that differentiates nanoparticles from traditional antibiotics. 45

### 3. 4. Determination of the Antifungal Activity of Silver Nanoparticles

The inhibition rates on fungal mycelial growth are also noteworthy. The 68.75% inhibition of *Fusarium solani* mycelial growth highlights the potential of VUAgNPs against fungal pathogens. This finding is consistent with previous studies suggesting that the efficacy of AgNPs against fungi may vary depending on the species of the microorganism.<sup>46</sup>

The 44.44% inhibition of *Aspergillus flavus* mycelial growth is also an important finding. However, the mycelial growth of *Aspergillus niger* was inhibited by only 6.66%. This suggests that silver nanoparticles may be less effective against certain fungal species. Additionally, the literature indicates that *Aspergillus* species generally exhibit resistance to silver nanoparticles and that the mycelial structure

Table 1. Determination of antimicrobial effect by line method

	Staphylococcus aureus	Staphylococcus mutans	Escherichia coli	Pseudomonas aeruginosa	Listeria monocytogenes	Candida sp
VUAgNPs	10	5	3	5	_	4

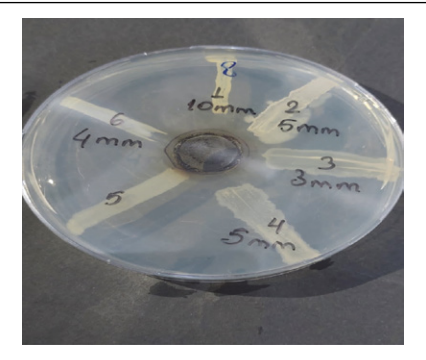


Table 2. % inhibition of samples on fungal mycelial growth

	Penicilium citrinum	Aspergillus flavus	Fusarium solani	Aspergillus niger
	NRRL174127	NRRL980	NRRL13414	1094
VUAgNPs	22,22	44,44	68,75	6,66

of these species may hinder the penetration of nanoparticles.<sup>47</sup> Monteiro et al.<sup>48</sup> reported that silver nanoparticles are particularly effective against soil-borne pathogens like *Fusarium* and that these nanoparticles damage fungal cell membranes. However, the low inhibition rate against *Aspergillus niger* (6.66%) may indicate the potential for some fungal species to develop resistance to VUAgNPs. This observation aligns with other studies highlighting the variable effectiveness of VUAgNPs against different fungal species.<sup>49</sup>

#### 4. Conclusion

This study successfully demonstrated the green synthesis of silver VUAgNPs using *V. uschakense* extract, an endemic medicinal plant, and evaluated their physicochemical characteristics alongside antioxidant and antimicrobial properties. The formation of nanoparticles was confirmed through various analytical techniques, with UV-Vis spectroscopy indicating a distinct surface plasmon resonance (SPR) at 432 nm typically associated with spherical particles and TEM analyses revealing particle sizes between 4–14 nm. These results affirm that the synthesized nanoparticles possess uniform morphology and high purity.

In terms of biological activity, VUAgNPs exhibited noteworthy free radical scavenging activity, particularly in the ABTS assay, although their antioxidant potential remained lower than that of the plant extract alone. More significantly, the nanoparticles displayed potent antimicrobial efficacy, completely inhibiting *Listeria monocytogenes* and exhibiting broad-spectrum activity against both Gram-positive and Gram-negative bacteria, as well as select fungal species such as *Fusarium solani*.

These findings highlight the dual value of *V. uschakense*: not only as a sustainable source for nanoparticle synthesis but also as a contributor to the development of bioactive nanomaterials with practical applications. Much like a bridge connecting nature and nanotechnology, this approach exemplifies how traditional medicinal plants can be harnessed for modern biomedical and food safety innovations. Future studies should delve deeper into the mechanistic pathways of these nanoparticles, their interaction with microbial membranes, and their potential cytotoxicity in clinical models, thereby advancing their applicability in therapeutic and preservative fields.

#### Acknowledgements

The authors are very grateful to Prof. Dr. Safiye Elif Korcan (Uşak University) for providing laboratory facilities and antimicrobial and antifungal activity studies.

#### **Conflict of interest:**

The authors report that there is no potential conflict of interest to declare

#### 5. Reference

- J. M. Iravani, S. Sharma, R. M. Balakrishnan, J. Hazard. Mater. 2017, 324, 54–61. DOI:10.1016/j.jhazmat.2016.11.021
- I. Khan, K. Saeed, I. Khan.. Arab. J. Chem. 2019, 12: 908–931.
   DOI:10.1016/j.arabjc.2017.05.011
- 3. S. Kumari, M. Tyagi, S. Jagadevan, *Int. J. Environ. Sci. Technol.* **2019**, *16*: 1–16. DOI: 10.1007/s13762-019-02468-3
- J. Jeevanandam, Y. S. Chan, M. K. Danquah. Chem. Bio. Eng. Rev., 2016, 3: 55–67. DOI:10.1002/cben.201500018
- S. Iravani, *Green Chem.*, 2011, 13: 2638–2650.
   DOI:http://dx.doi.org/10.1039/c1gc15386b
- A. F. Burlec, A. Corciova, M. Boev, D. Batir-Marin, C. Mircea,
   O. Cioanca, G. Danila, M. Danila, A. F. Bucur, M. Hancianu,
   Pharmaceuticals, 2023, 16: 1410. DOI:10.3390/ph16101410.
- 7. M. G. S. S. Al-Asbahi, B. A. Al-Ofiry, F. A. A. Saad, et al., Sci Rep, 2024, 14: 10224. DOI:10.1038/s41598-024-59936-1.
- 8. H. I. M. Amin, F. H. S. Hussain, G. Gilardoni, Z. M. Thu, M. Clericuzio, G. Vidari, *Plants*, **2020**, *9*: 1066.
   **DOI:**10.3390/plants9091066
- 9. N. H. Doğru, N. Demir, Ö. Yılmaz, *Turk. J. Anal. Chem.*, 2021, 3: 19–26. DOI:10.51435/turkjac.886692
- P. Donn, P. Barciela, A. Perez-Vazquez, L. Cassani, J. Simal-Gandara, M. A. Prieto, *Biomolecules*, 2023, 13: 427.
   DOI:10.3390/biom13030427
- 11. J. M. Geyesa, T. B. Esho, B. A. Legesse, A. S. Wotango, *Heli-yon*, **2024**, 10: e24215. **DOI:**10.1016/j.heliyon.2024.e24215
- M. R. Kıvanç, J. Macromol. Sci. A, 2022, 59: 828–837.
   DOI:10.1080/10601325.2022.2140676
- Ö. Hazman, G. Khamidov, M. A. Yilmaz, M. F. Bozkurt, M. Kargioğlu, D. Tukhtaev, I. Erol, *Environ. Sci. Pollut. Res. Int.*, 2024 31: 33482–33494. DOI:10.1007/s11356-024-33424-5.
- 14. İ. İ Tatli., Z. Ş. Akdemir, Fabad Journal of Pharmaceutical Sciences, 2006, 31:85–96.
- N. Krithiga, A. Rajalakshmi, A. Jayachitra, *J. Nanosci.* 2015, 8, 928204. DOI:10.1155/2015/928204
- S. Pirtarighat, M. Ghannadnia, S. Baghshahi, J. Nanostruct. Chem. 2019, 9: 1–9. DOI:10.1007/s40097-018-0291-4
- 17. M. Naveed, B. Bukhari, T. Aziz, S. Zaib, M. A. Mansoor, A. A. Khan, M. Shahzad, A. S. Dablool, M. W. Alruways, A. A. Almalki, *Molecules.* 2022, 27: 4226. DOI:10.3390/molecules27134226
- 18. M. Blois, *Nature*, **1958**, 181:1199–1200. **DOI:**10.1038/1811199a0
- P. D. Duh, W. J. Yen, C. Du, G. C. Yen, J. Am. Oil Chem. Soc..
   1997, 74: 1059–1063. DOI:10.1007/s11746-997-0025-0
- 20. M. Burits, K. Asres, F. Bucar, *Phytother Res.*, **2001**, *15*: 103–108. **DOI**:10.1002/ptr.691
- 21. K. Thaipong, U. Boonprakob, K. Crosby, L. Cisneros-Zevallos, D. H. Byrne, *J. Food Compos. Anal.*, **2006**, 19: 669–675. **DOI:**10.1016/j.jfca.2006.01.003.
- 22. K. O. Saygi, H. M. Bayram, E. Bayram, *Biomass Conv. Bioref.*, **2024**, 14: 5531–5539. **DOI:**10.1007/s13399-022-02857-8
- Y. G. Sun, Y. Xia, Science, 2002, 298: 2176–2179.
   DOI:10.1126/science.1077229
- 24. K. L. Kelly, E. Coronado, L. L. Zhao, G. C. Schatz, J. Phys.

- Chem. B., **2003**, 107: 668–677. **DOI:**10.1021/jp026731y
- P. K. Jain, K. S. Lee, I. H. El-Sayed, M. A. El-Sayed, J. Phys. Chem. B., 2006, 110: 7238–7248. DOI:10.1021/jp0571700
- N. Tarannum, Divya, Y. K. Gautam, RSC Advances, 2019, 9: 34926–34948. DOI:10.1039/c9ra04164h
- X.-F. Zhang, Z.-Liu, G. Shen, W. S. Gurunathan, *Int. J. Mol. Sci.*, 2016, 17: 1534. DOI:10.3390/ijms17091534
- S. Pal, Y. K. Tak, J. M. Song. Appl. Environ. Microbiol. 2007, 73:1712–1720. DOI:10.1128/AEM.02218-06
- K. V. Sharma, A. R. Yngard, Y.Lin, Adv. Colloid. Interface.
   Sci., 2009, 145: 83–96. DOI:10.1016/j.cis.2008.09.002.
- M. M. Alanazi, J. King, Saud. Univ. Sci., 2024, 36:103312, DOI:10.1016/j.jksus.2024.103312
- 31. G. A Sotiriou, S. E Pratsinis, *Curr. Opin. Chem. Eng.* **2011**, 1:3–10, **DOI**:10.1016/j.coche.2011.07.001
- 32. M. Ahamed, M. S. Alsalhi, M. K. Siddiqui. *Clin. Chim. Acta.* **2010**, 411:1841–1848. **DOI**:10.1016/j.cca.2010.08.016
- 33. A. M. Awwad, N. M. Salem, A. O. Abdeen, *Int. J. Ind. Chem.*, **2013**, 4, 29 **DOI**: 10.1186/2228-5547-4-29
- G. Bagherzade, M. M. Tavakoli, M. H. Namaei, *Asian Pac. J. Trop. Biomed.*, 2016, 7, I 3, 227–233,
   DOI:10.1016/j.apjtb..12.014
- T. Imtiaz, R. Priyadharshini, S. Rajeshkumar, P. Sinduja, J. Pharm. Res. Int. 2021, 33(51A), 342–352.
   DOI:10.9734/jpri/2021/v33i51A33501
- V. R. Netala, M. S. Bethu, B. Pushpalatha, *Int. J. Nanomedicine.*, 2016, 11, 5683–5696. DOI:10.2147/IJN.S112857.
- 37. A. K. Biswal, P. K. Misra, *Mater. Chem. Phys.*, **2020**, 123014, **DOI:**10.1016/j.matchemphys.2020.123014

- 38. İ. A. Balkan, T. Taşkın, H. T. Doğan, İ. Deniz, G. Akaydın, E. Yesilada, *Ind. Crops. Prod.*, **2017**: 95, 95–703,
- DOI:10.1016/j.indcrop.2016.11.038.
- F. Ö. Küp, S. Çoşkunçay, F. Duman, Mater. Sci. Eng. C., 2019, 110207, DOI: 0.1016/j.msec.2019.110207.
- R. Re, N. Pellegrini, A. Proteggente, A. Pannala, M. Yang,
   C. Rice-Evans Free Radic Biol. Med., 1999, 26:1231–1237.
   DOI:10.1016/s0891-5849(98)00315-3
- 41. R. L. Prior, X. Wu, K. Schaic. *J. Agric. Food Chem.* **2005**, 53: 4290–4302. **DOI**:10.1021/jf0502698
- M. Rai, A. Yadav, A. Gade. *Biotechnol. Adv.* 2009, 27: 76–83.
   DOI:10.1016/j.biotechadv.2008.09.002
- 43. X. Chen, H. J. Schluesener, *Toxicol. Lett.* **2008**, 176: 1–12, **DOI:**10.1016/j.toxlet.2007.10.004.
- J. R. Morones-Ramirez, J. A. Winkler, C. S. Spina, J. J. Collins, Sci. Transl. Med. 2013,5:190ra81.
   DOI:10.1126/scitranslmed.3006276
- S. Shrivastava, T. Bera, A. Roy, G. Singh, P. Ramachandrarao,
   D. Dash, *Nanotechnol.*, 2007, 18: 225103.
   DOI:10.1088/0957-4484/18/22/225103
- 46. M. Gajbhiye, J. Kesharwani, A. Ingle, A. Gade, M. Rai, *Nanomedicine*. **2009**;5:382–386. **DOI**:10.1016/j.nano.2009.06.005
- K. J. Kim, W. S. Sung, B. K. Suh, S. K. Moon, J. S. Choi, J. G. Kim, D. G. Lee, *Biometals*, 2007, 20: 191–198.
   DOI:10.1007/s10534-008-9159-2
- D. R. Monteiro, L. F. Gorup, A. S. Takamiya, A. C. Ruvollo-Filho, E. R. de Camargo, D. B. Barbosa, *Biofouling*, 2009, 9: 4967–4970. DOI:10.1080/08927014.2011.599101
- K. J. Kim, S. N. Park, S. S. Kim, S. H. Kim, Nanotechnology,
   2012, 23:115101. DOI:10.1088/0957-4484/23/11/115101

#### Povzetek

Nanodelce srebra, sintetizirane z uporabo ekstrakta *Verbascum uschakense* pri reakcijski temperaturi 60 °C, smo karakterizirali z različnimi analitskimi metodami. Te so vključevale UV-vis absorpcijsko spektroskopijo, rentgensko difrakcijsko analizo (XRD), visoko ločljivo presevno elektronsko mikroskopijo (HR-TEM) ter vrstično elektronsko mikroskopijo (SEM) v kombinaciji z energijsko disperzijsko rentgensko spektroskopijo (EDX). Spektroskopska analiza je pokazala značilen vrh pri valovni dolžini 432 nm, kar potrjuje uspešno tvorbo srebrovih nanodelcev (AgNP). Mikroskopske analize so pokazale, da so bili nanodelci pretežno sferične oblike, z velikostjo delcev med 4 in 14 nm. Rentgenska difrakcijska analiza je potrdila ploskovno centrirano kubično (FCC) kristalno strukturo nanodelcev, kar se je odražalo v značilnih difrakcijskih vrhovih pri 2θ vrednostih 38,21°, 44,46°, 64,59° in 77,48°, ki ustrezajo kristalnim ravninam (111), (200), (220) in (311).

Glede biološke aktivnosti smo antioksidativno sposobnost vodnega ekstrakta *V. uschakense* ovrednotili kot sposobnost odstranjevanja prostih radikalov. Pri koncentraciji 1 mg/mL je ekstrakt izkazal 86,93 % inhibicije stabilnega radikala 2,2-difenil-1-pikrilhidrazil (DPPH). V primerjavi s tem so srebrovi nanodelci, sintetizirani iz istega rastlinskega ekstrakta, pri enaki koncentraciji dosegli 60,04 % inhibicijo DPPH radikala. Poleg tega so AgNP v ABTS testu (2,2'-azino-bis(3-etilbenzotiazolin-6-sulfonska kislina)) pokazali izrazito antioksidativno aktivnost, primerljivo z rezultati, doseženimi z uporabo standardnega antioksidanta Trolox.

Antimikrobne lastnosti biosintetiziranih srebrnih nanodelcev smo preučevali z metodo difuzije na disku. Nanodelci so izkazovali inhibicijsko delovanje proti več patogenim mikroorganizmom, vključno z vrstami *Staphylococcus aureus*, *Streptococcus mutans*, *Escherichia coli*, *Pseudomonas aeruginosa*, *Listeria monocytogenes* in glivami iz rodu *Candida*.

Ti rezultati poudarjajo potencial srebrnih nanodelcev, sintetiziranih s pomočjo *V. uschakense*, kot večnamenskih bioaktivnih agensov z antioksidativnimi in antimikrobnimi lastnostmi. Študija dokazuje, da zelena sinteza predstavlja trajnosten in učinkovit pristop k pripravi nanomaterialov z možnimi aplikacijami na področjih biomedicine in farmacije.



Except when otherwise noted, articles in this journal are published under the terms and conditions of the Creative Commons Attribution 4.0 International License